SUPPORTING INFORMATION

Perovskite phase formation in pure and Sm- and La-substituted $BiFeO_3$ thin films under isothermal and non-isothermal regimes

M. A. M Teixeira[1], F. B. Minussi[1*], J. A. Eiras[2], E. B. Araújo[1]

[1] Department of Physics and Chemistry, São Paulo State University, 15385-007, Ilha Solteira, SP - Brazil

[2] Department of Physics, Federal University of São Carlos, 13565-905, São Carlos, SP - Brazil

CONTENTS

* corresponding author: fbminussi@gmail.com

Supplementary Note 1: Cross-section SEM images

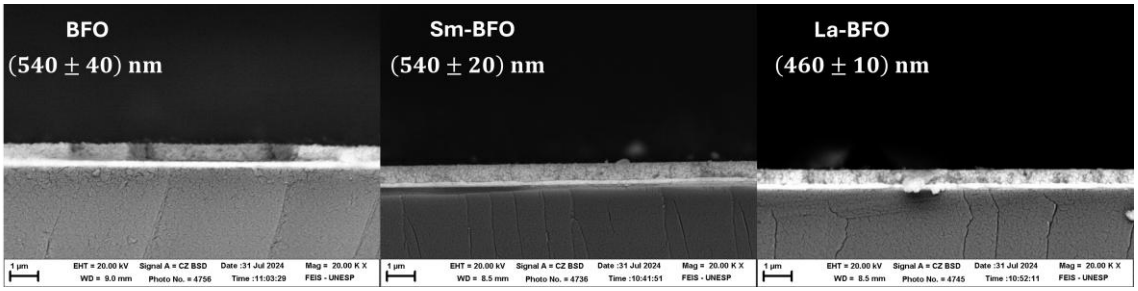

Figure S1 - Cross-section SEM images of the bismuth ferrite-based thin films. Deviation calculated through the standard deviation based on 8 different measurements.

Supplementary Note 2: Time-dependent XRD data of samples treated at 600 °C

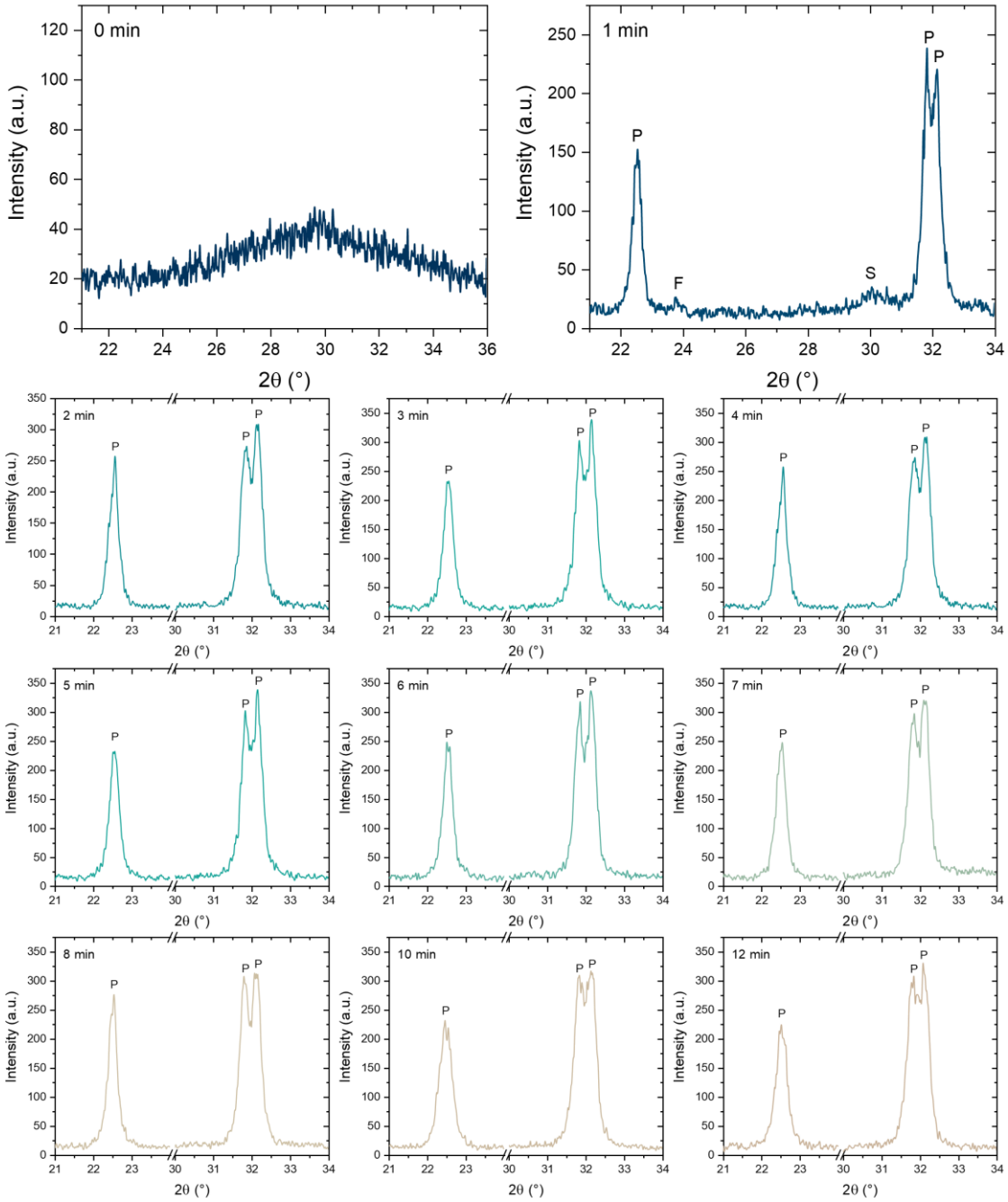

Figure S2 - X-ray diffraction data of pure BFO thin films thermal annealed at 600 °C for different times. P, F, and S are peaks related to perovskite, ferrite, and sillenite phases, respectively.

Supplementary Note 3: Structure and XRD profiles of analyzed phases

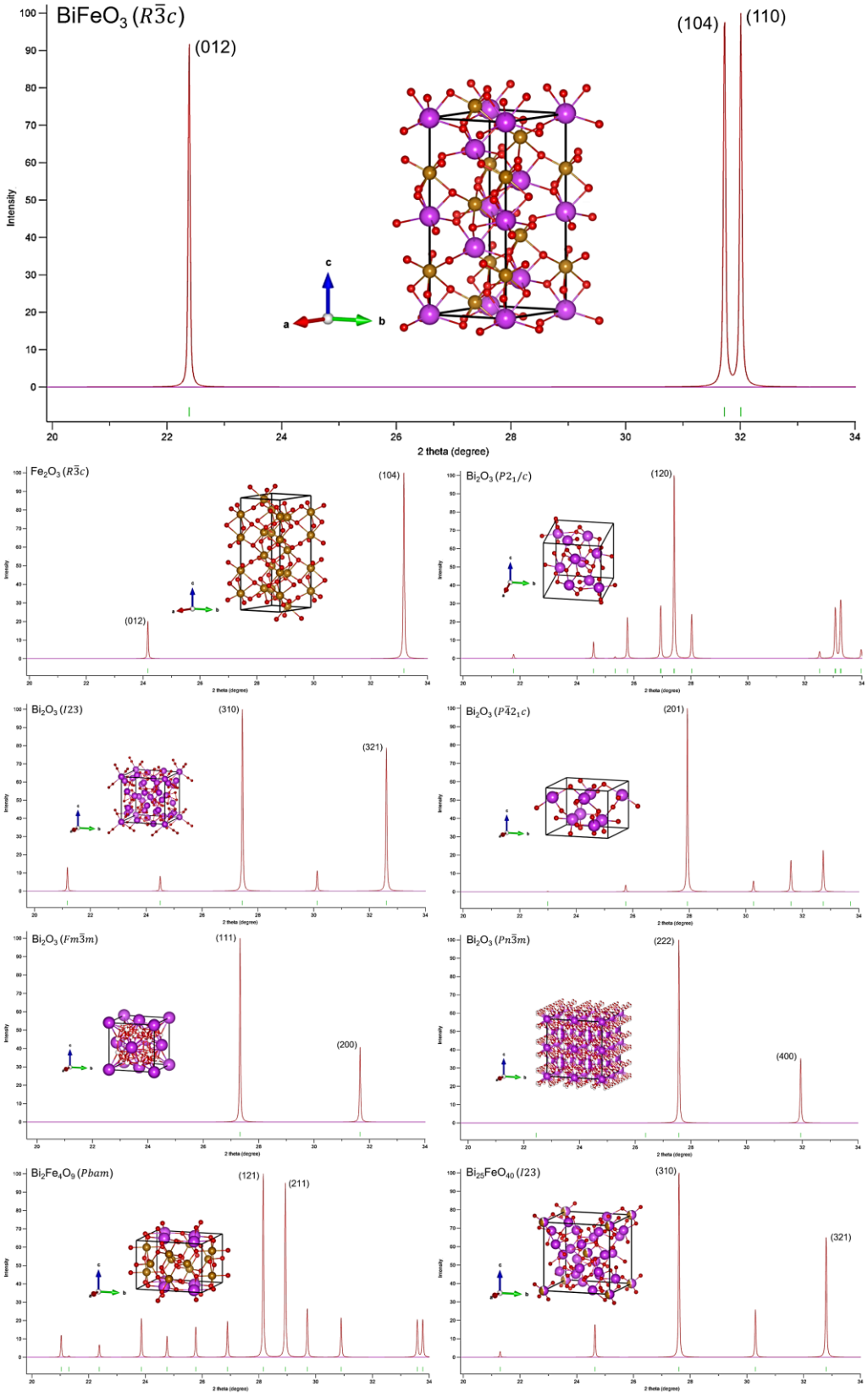

Figure S3 - Theoretical diffractograms, space groups, and idealized structures of the different compounds that can be formed during the synthesis of BFO-based materials. XRD profiles and structures were generated using VESTA.

Supplementary Note 4: Atomic force microscopy measurements

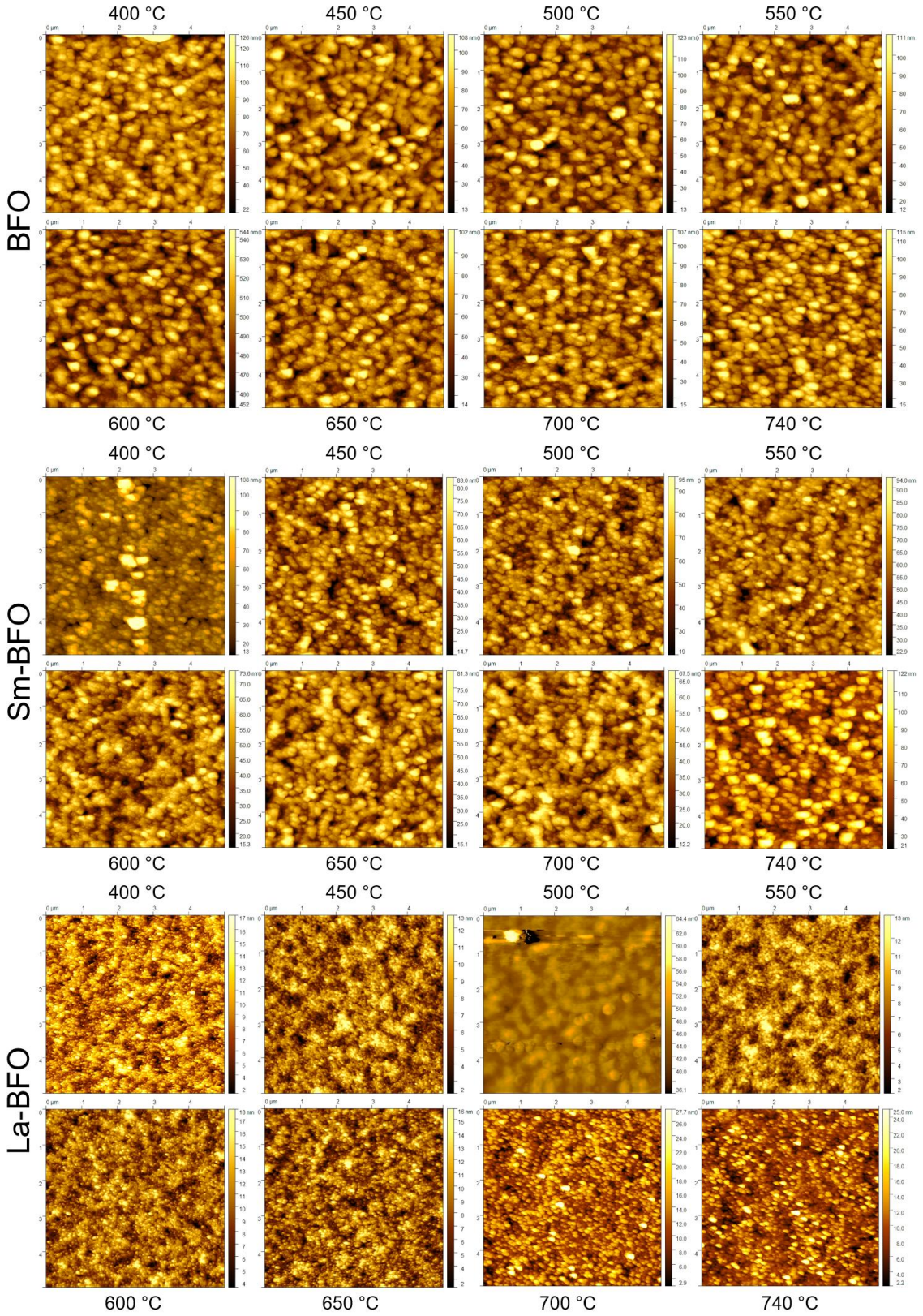

Figure S4 - Atomic force microscopy images of the films submitted to the non-isothermal regime.

Supplementary Note 5: Summary of the tested theoretical models

Table S1 - Integral functions of reaction kinetic models tested to fit the experimental data collected under non-isothermal conditions.

Group	Model	Symbol	$g(\alpha)$
Nucleation	Second-order power law	P2	$\alpha^{1/2}$
	Third-order power law	P3	$\alpha^{1/3}$
	Fourth-order power law	P4	$\alpha^{1/4}$
	Avrami-Erofeyev	A2	$[-\ln(1-\alpha)]^{1/2}$
		A3	$[-\ln(1-\alpha)]^{1/3}$
		A4	$[-\ln(1-\alpha)]^{1/4}$
Geometrical contraction	Contracting area	R2	$1-(1-\alpha)^{1/2}$
	Contracting volume	R3	$1-(1-\alpha)^{1/3}$
Diffusion	1D diffusion	D1	α^2
	2D diffusion	D2	$[(1-\alpha)\ln(1-\alpha)]+\alpha$
	3D diffusion	D3	$[1-(1-\alpha)^{1/3}]^2$
Reaction order	First-order	F1	$-\ln(1-\alpha)$
	Second-order	F2	$[1/(1-\alpha)]-1$
	Third-order	F3	$(1/2)[(1-\alpha)^{-2}-1]$

Supplementary Note 6: Fits of experimental data

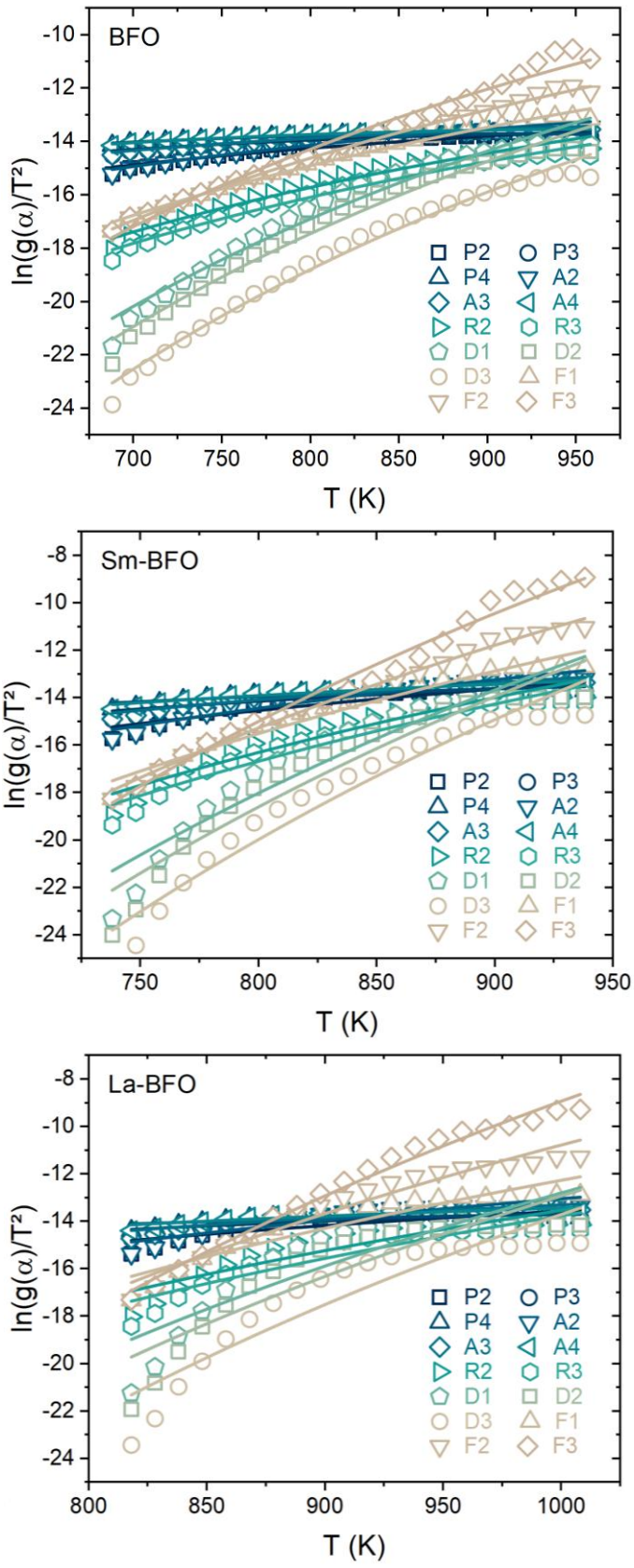

Figure S5 - Experimental data converted to $\ln[g(\alpha)/T^2]$ using each of the models shown in Table S1 and respective fits with the Coats-Redfern approximation.

Supplementary Note 7: Arrhenius parameters obtained with all kinetic models

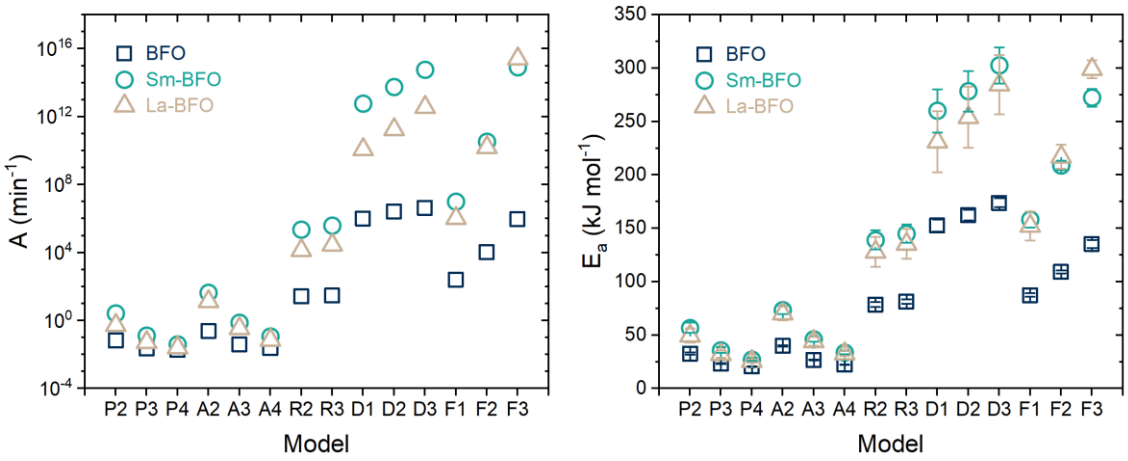

Figure S6 - Pre-exponential constant and activation energies obtained with each kinetic model for the studied BFO-based thin films. Error bars are the fit residuals.